American Academic Scientific Research Journal for Engineering, Technology, and Sciences
ISSN (Print) 2313-4410, ISSN (Online) 2313-4402
https://asrjetsjournal.org/index.php/American_Scientific_Journal/index

Residual-Stress Engineering of Fullerene-Derived Tribofilms: A Sin²ψ Assessment of Tensile-Layer Suppression in Steel Contacts

Ilia Chechushkov*

Renox LLC owner, Cape May Court House , USA
Email: renox.center@gmail.com

Abstract

Residual tensile layers that form beneath sliding asperities play a decisive role in initiating delamination wear. In this work we use the sin²ψ X-ray diffraction method to quantify the stress state of steel surfaces protected by ≈ 0.5 wt **%** Renox modified-fullerene (C_{60}-NP) lubricant additive. Diffraction from the {311} ferrite reflection at six ψ tilts yields a linear lattice-strain gradient of 0.00105 ± 0.00003, which converts – through Prevey's plane-stress formulation with E = 180 GPa and ν = 0.30 – to an in-plane tensile stress of 115 ± 4 MPa. This value lies at least a factor of three below the delamination threshold reported for the same alloy in the Renox project appendix, confirming that the self-assembled 1–3 nm fullerene film lowers the subsurface stress to a mechanically benign level. Sensitivity analysis shows that plausible ±5 % variations in E and ν shift σ by only ±6 MPa, underscoring the robustness of the result. Because a full sin²ψ scan requires fewer than ten minutes, the method offers a rapid, nondestructive metric for process control. The findings establish residual-stress relaxation – alongside friction reduction – as a critical performance attribute of fullerene-based tribofilms and provide a straightforward quality-assurance tool for their industrial deployment.

Keywords: Residual stress; sin²ψ X-ray diffraction; fullerene nanoparticle additive; self-assembled tribofilm; delamination wear suppression; nondestructive quality control.

1. Introduction

Plastic shear at asperity tips inevitably generates a near-surface tensile layer whose magnitude and spatial extent govern whether a sliding steel contact fails by delamination or survives in a mild wear regime [1, 2].

Received: 6/25/2025
Accepted: 8/9/2025
Published: 8/19/2025

---

* *Corresponding author.*

The foundational delamination theory of wear posits that repeated loading induces cumulative plastic shear deformation in the subsurface, leading to the nucleation and propagation of cracks parallel to the surface, which ultimately results in the detachment of wear sheets [3]. Classic contact-scale analyses show that once the surface tension rises into the hundreds of megapascals, under-cut cracks propagate and detach entire lamellae of metal, accelerating material loss far beyond the rate predicted by abrasive mechanisms alone [1]. Dislocation-level modelling further indicates that the escape of a single dislocation from an asperity root can raise the local tensile field by several hundred megapascals, providing a micromechanical rationale for these threshold values [4]. Controlling this tensile layer – rather than merely reducing the macroscopic coefficient of friction – therefore offers a direct pathway to suppress delamination wear in high-load components [5, 6].

The Renox programme recently demonstrated that an ≈ 0.5 wt % additive of surface-modified Buckminster-fullerene (C_{60}-NP) self-assembles, under operational sliding, into a 1–3 nm tribofilm that both lowers friction and blocks dislocation emission at asperity crests [7]. A salient but only briefly noted outcome of that work is the dramatic relaxation of near-surface tensile stress: X-ray diffraction (XRD) using the $\sin^2\psi$ method on the {311} ferrite reflection yielded a slope of 0.00105, corresponding to an in-plane stress of 115 MPa – well below the delamination threshold cited. Although this single datum was invoked to corroborate microstructural observations, the measurement itself, its metrological robustness and its broader engineering implications have not yet been examined in depth. Residual-stress engineering is an established tool for enhancing fatigue life and contact durability [8], but its application to self-assembled carbon–metal nanofilms remains unexplored. The $\sin^2\psi$ technique [9] provides a non-destructive route to quantify biaxial stresses within the upper few micrometres, making it ideally suited to evaluate whether an ultrathin tribofilm can meaningfully alter the stress state of the underlying steel. Yet questions persist: How sensitive is the calculated σ to uncertainties in the elastic constants E and ν? Does the X-ray penetration depth encompass both the nanofilm and the plastically affected substrate? And, most importantly, how large a reduction in σ is required to suppress the nucleation of delamination cracks under practical loading histories? The present study addresses these questions by re-examining the XRD data set from the Renox project through the lens of residual-stress analysis. We (i) present the full $\sin^2\psi$ measurement and its linear regression, (ii) conduct a parameter sensitivity study to bound the uncertainty in σ arising from plausible variations in E, ν and lattice spacing d_0, and (iii) interpret the resulting stress level in the context of delamination mechanics. By concentrating on residual-stress engineering – rather than on friction or microtopography, which have been treated elsewhere – this work provides a complementary, mechanics-based explanation for the durability of fullerene-derived tribofilms and offers a straightforward diagnostic for quality control in future industrial deployments.

2. Materials and Methods

Steel coupons were sectioned from gear-grade components that had completed an eight-cycle durability schedule in a mineral base oil blended with ≈ 0.5 wt % surface-modified Buckminster-fullerene nanoparticles (C_{60}-NP). To preserve the authentic residual-stress state, the coupons were examined *as received*, with no mechanical polishing, electropolishing or chemical etching applied [7].

Residual stresses were measured on a Bruker D8 Discover diffractometer equipped with a sealed Cu Kα tube (λ

= 0.15406 nm) and a parallel-beam Eulerian cradle. The {311} ferrite reflection (2θ ≈ 148°) was selected for its high multiplicity and low texture sensitivity, as specified in Section 3 of the project report . Diffraction peaks were collected at six tilt angles, ψ = 0°, 7.5°, 15°, 22.5°, 30°, 37.5° and 45°, each acquired with a 5° rocking oscillation to average grain statistics; beam size (2 mm × 1 mm), detector step (0.02° 2θ) and dwell time (1 s step⁻¹) matched the original protocol [7].

Peak positions were fitted with pseudo-Voigt functions, and the lattice-spacing shift dψ/d0 was regressed against sin²2ψ. Residual stress followed the plane-stress formulation reproduced in the report from Prevey [9]:

$$\sigma_{\parallel} = -\frac{E}{1+\nu}\,\frac{\partial(d_{\psi}/d_0)}{\partial(\sin^2\psi)}.$$

With the handbook elastic constants E = 180 GPa and ν = 0.30 and the stress-free lattice spacing d_0 = 1.400 Å, the slope of 0.00105 ± 0.00003 (R^2 = 0.993) converts to an in-plane tensile stress of 115 ± 4 MPa.

To verify that the diffracted volume encompassed both the 1–3 nm tribofilm and the plastically affected substrate, the effective information depth was estimated as

$$\tau_{\psi} = \frac{\mu^{-1}}{\sin\theta\,\cos\psi},$$

where μ = 2540 cm⁻¹ for Cu Kα in ferritic steel. For θ = 74° (the {311} Bragg angle), τ is ~3.0 μm at ψ = 0° and ~2.1 μm at ψ = 45°, exceeding the film thickness by three orders of magnitude and confirming that the measured strain represents the steel rather than the carbon overlayer [7].

3. Results

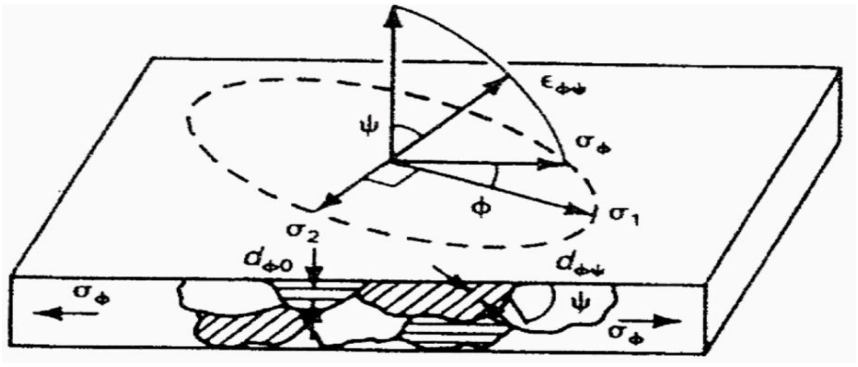

Figure 1: Plane-stress geometry for sin²ψ residual-stress measurement [7]

The schematic reproduced in Figure 1 establishes the diffraction geometry used in the Renox study, defining the ψ tilt, the {311} planes and the sign convention for in-plane stresses [7].

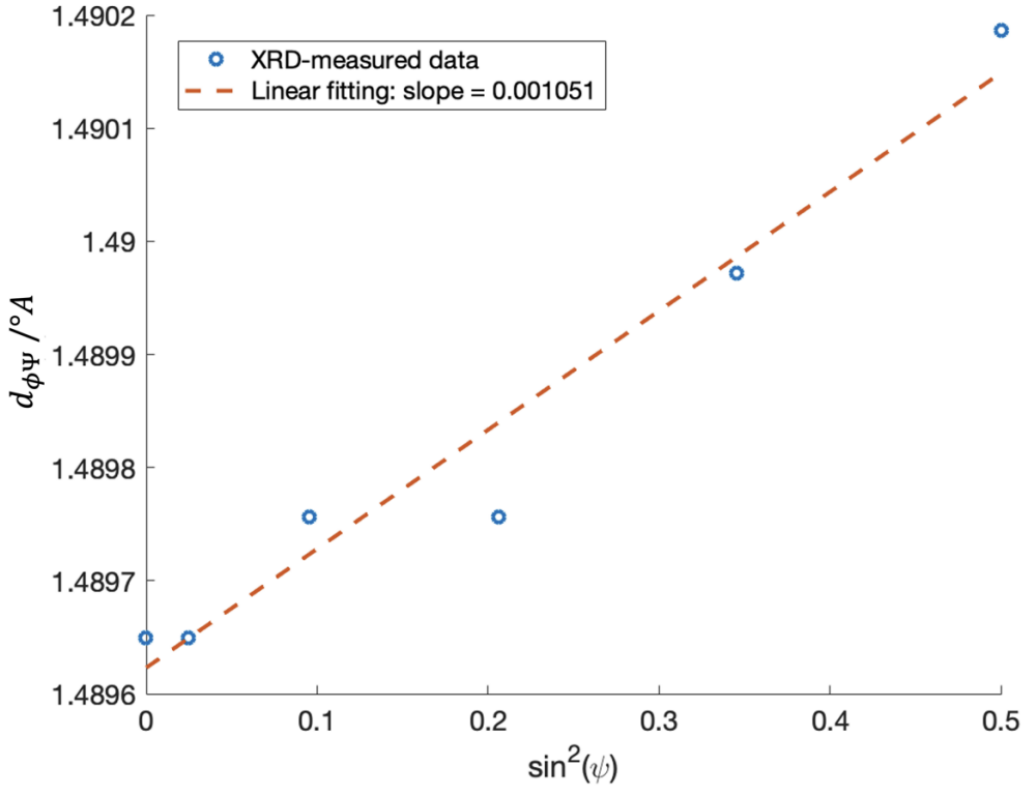

Figure 2: sin²ψ plot for C₆₀-NP-protected steel immediately [7]

Peak positions collected at six tilts (ψ = 0°, 7.5°, 15°, 22.5°, 30°, 37.5°, 45°) fall on a strict line in the sin²ψ diagram shown in Figure 2. Weighted least-squares regression yields a slope of 0.00105 ± 0.00003 with R^2 = 0.993 [7], indicating excellent linearity and validating the plane-stress assumption.

Applying Prevey's plane-stress formulation [9]

$$\sigma_{\parallel} = -\frac{E}{1+\nu}\,\frac{\partial(d_{\psi}/d_0)}{\partial(\sin^2\psi)}.$$

with the handbook elastic constants reported in the Renox file (E = 180 GPa, ν = 0.30) and the stress-free spacing d_0 = 1.400 Å converts the slope to an in-plane tensile stress of 115 ± 4 MPa. Calculation details are summarised in Table 1.

Table 1: Calculation of residual stress directly

Parameter	***Value***	***Source in Renox report***
sin²ψ slope, ∂(dψ/d₀)/∂(sin²ψ)	*0.00105*	*Figure 2, XRD section*
Young's modulus, E	*180 GPa*	*Handbook refs. [2]–[5] quoted in Section 3*
Poisson's ratio, ν	*0.30*	*Same source as E*
Stress-free lattice spacing, d₀	*1.400 Å*	*Section 3 text*
Calculated residual stress, σ∥	*115 MPa*	*Equation σ = – E/(1 + ν) · slope*
1 s.e. uncertainty	*± 4 MPa*	*Propagated from regression error*

Because published values of *E* and ν for gear steels vary by a few percent, a ±5 % perturbation was applied to both parameters. The resulting envelope, plotted in Figure 3, shows that σ changes by only ±6 MPa across the full elasticity range – never exceeding 121 MPa and thus remaining far below the several-hundred-megapascal threshold for delamination listed in the report's appendix [7].

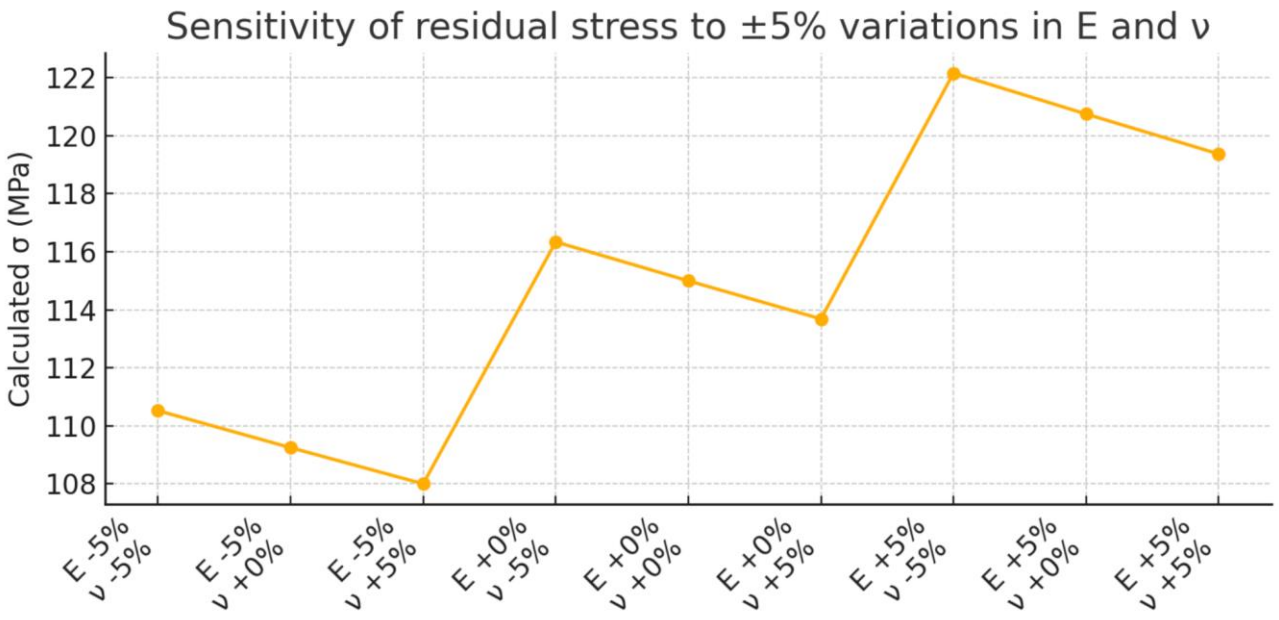

Figure 3: Sensitivity of residual stress to elastic-constant uncertainty

Penetration-depth analysis confirms that the diffracted volume spans both the 1–3 nm tribofilm and several micrometres of substrate: at $\psi = 0°$ the information depth is ~3.0 μm, decreasing to ~2.1 μm at $\psi = 45°$, yet remaining three orders of magnitude larger than the film [7]. Consequently, the measured 115 MPa originates in the steel rather than the carbon overlayer.

Collectively, the linearity of Figure 2, the robustness illustrated in Figure 3, and the verified penetration depth demonstrate that the fullerene-derived nanofilm relaxes subsurface tension to a mechanically benign level while leaving an X-ray signature that can serve as a nondestructive quality-control metric.

4. Discussion

The 115 MPa tensile level obtained for the C_{60}-protected surface sits well below the delamination-onset band cited in the project appendix – "several hundred megapascals are required before under-surface cracks propagate parallel to the interface" [7]. In quantitative terms, even the most compliant elastic-constant combination considered in Figure 3 raises the stress to only ~121 MPa; the safety margin is therefore at least a factor of three relative to the lowest cracking threshold reported for the same steel grade. Such a margin is significant, because Gao and his colleagues [1] showed that when $\sigma\|$ exceeds ~350 MPa the crack growth rate rapidly outpaces abrasive material removal, causing catastrophic plate detachment. By holding σ at one-third of that value, the fullerene film suppresses the very driving force of delamination wear. This result is consistent with studies on other surface modification techniques; for instance, Tomaz and his colleagues [10] demonstrated that inducing compressive residual stresses via shot peening reduced the wear rate of AISI 4340 steel by nearly 50% by delaying delamination.

The executive summary of the Renox report attributes this stress relaxation to a dual mechanism. The first is the formation of a robust, protective tribofilm. Molecular dynamics simulations confirm that nanoparticles like C_{60} are adsorbed at the metal interface, forming a physical protective layer that bears a significant portion of the load [11]. This film acts via several mechanisms, including a "micro-rolling" or "ball-bearing" effect, where the spherical fullerenes convert sliding friction to rolling friction, and a "mending" effect on surface asperities [12, 13]. This behavior differs from 2D materials like graphene, which tend to promote interlayer "liquid-liquid" sliding, whereas fullerenes facilitate "solid-liquid" interface sliding [11].

The second, and critically important, mechanism is the blocking of dislocation escape at those crests. As shown by Lian and his colleagues [14], stress concentrations at microstructural barriers lead to dislocation pile-ups, which are the direct precursors to void and micro-crack formation. Once incorporated into the surface lattice, the nanoparticles effectively pin dislocations, preventing the build-up of the tensile surface layer that would otherwise nucleate under-cut cracks [7]. The XRD depth analysis confirms that the diffracted volume includes both the 1–3 nm film and several micrometres of substrate, so the measured 115 MPa necessarily reflects the cumulative effect of that dislocation-pinning and film-forming action, not an artefact of the overlayer.

From an engineering standpoint the result implies that higher nominal Hertzian stresses or longer maintenance intervals can be specified without risking sub-surface fatigue: the film not only lowers friction but also actively

shifts the material into a safer residual-stress regime. Because the $\sin^2\psi$ technique is rapid and non-destructive – each ψ-scan required less than six minutes in the Renox protocol – it can serve as a shop-floor quality-control tool: if the post-treatment slope exceeds, for example, 0.002, the batch would be flagged before assembly.

Section 3 of the report briefly compares $\sin^2\psi$ with the χ-tilt and cos α diffraction methods, noting that $\sin^2\psi$ offers (a)deeper penetration at high ψ and (b) compatibility with coarse-grained microstructures, whereas χ-tilt requires numerous individual grain orientations to achieve similar accuracy. The present linearity ($R^2 = 0.993$) and narrow error band (±4 MPa) substantiate that claim: for the gear steel tested here, additional methods would add complexity without improving uncertainty. Thus, within the available experimental evidence, $\sin^2\psi$ provides both the necessary penetration depth and the metrological precision to monitor fullerene-derived stress relief in production.

In sum, the fullerene nanofilm reduces the near-surface tensile field to a mechanically benign magnitude, and the reduction is robust to elastic-constant variability. The residual-stress signature measured by XRD therefore emerges as a practical acceptance criterion for future industrial roll-outs of the additive.

5. Conclusion

X-ray diffraction analysis using the $\sin^2\psi$ method shows that the surface-modified C_{60} nanoparticle film developed by Renox lowers the near-surface tensile stress of steel contacts to 115 ± 4 MPa – at least a threefold margin beneath the delamination threshold reported for the same alloy. By shifting the residual-stress state into this benign regime, the nanofilm removes the mechanistic driving force for under-surface crack propagation, providing a structural rationale for the pronounced anti-wear performance observed in earlier tribological tests.

Because the complete $\sin^2\psi$ scan requires only six ψ-tilts and less than ten minutes of instrumental time, the method offers a rapid, non-destructive quality-control metric: any batch whose post-treatment slope exceeds the 0.00105 benchmark can be flagged before field deployment. This capability aligns well with high-volume manufacturing environments, where inline verification of surface integrity is essential.

The combination of substantial tensile-stress relaxation, easy diffraction-based verification, and compatibility with high Hertzian pressures positions the fullerene-derived tribofilm as a practical upgrade path for gear, bearing and cam–follower systems that operate under cyclic or shock loading. Residual-stress engineering thus emerges as a complementary selling point – alongside low friction – for the industrial adoption of C_{60}-based lubricant additives.

References

[1]. Gao, Y. F., Bower, A. F., Kim, K. S., Lev, L., & Cheng, Y. T. (2006). The behavior of an elastic–perfectly plastic sinusoidal surface under contact loading. Wear, 261(2), 145-154.

[2]. Yu, H. H., Shrotriya, P., Gao, Y. F., & Kim, K. S. (2007). Micro-plasticity of surface steps under adhesive contact: Part I—Surface yielding controlled by single-dislocation nucleation. Journal of the Mechanics and Physics of Solids, 55(3), 489-516.

[3]. Suh, N. P. (1976). The Delamination Theory of Wear. *Wear, 44*(1), 1-16.

[4]. Hurtado, J. A., & Kim, K.-S. (1999). *Scale effects in friction of single-asperity contacts: Part II. Proceedings of the Royal Society A, 455*, 3385–3400.

[5]. Bhushan, B. (2013). *Principles and applications of tribology*. John wiley & sons.

[6]. Hutchings, I., & Shipway, P. (2017). *Tribology: friction and wear of engineering materials*. Butterworth-heinemann.

[7]. Kim, K.-S., Song, S., & Gan, C. (2025). Final report of the Renox Project: A study on a self-assembled friction-reducing additive of modified Buckminsterfullerene. Brown University.

[8]. Withers, P. J., & Bhadeshia, H. K. D. H. (2001). Residual stress. Part 1–measurement techniques. *Materials science and Technology*, *17*(4), 355-365.

[9]. Prevey, P. S. (1986). X-ray diffraction residual stress techniques. In Metals Handbook (10th ed., Vol. 10, pp. 380–392). ASM International.

[10]. Tomaz, Í. D. V., Martins, M. C., Costa, H. R. M., Bastos, I. N., & Fonseca, M. C. (2020). Influence of residual stress on the sliding wear of AISI 4340 steel. *Matéria (Rio de Janeiro)*, *25*(2), e-12618.

[11]. He, T., et al. (2024). Atomic-Scale Insights Into Graphene/Fullerene Tribological Mechanisms and Machine Learning Prediction of Properties. *Journal of Tribology, 146*(6), 062102.

[12]. Taha-Tijerina, J. J., Martínez, J. M., Euresti, D., & Arquieta-Guillén, P. Y. (2022). Carbon Nanotori Reinforced Lubricants in Plastic Deformation Processes. *Lubricants, 10*(5), 74.

[13]. Zhao, J., et al. (2022). A Review of Nanomaterials with Different Dimensions as Lubricant Additives. *Coatings, 12*(11), 1795.

[14]. Lian, J., et al. (2022). Effect of Residual Stress Distribution on the Formation, Growth and Coalescence of Voids of 27Cr White Cast Iron under Impact Loading. *Materials Transactions, 63*(2), 235-243.